POLITECNICO DI TORINO
Repository ISTITUZIONALE

Robustness of precipitation Emergent Constraints in CMIP6 models

Terms of use:

Publisher copyright

(Article begins on next page)

17 May 2024

Robustness of precipitation Emergent Constraints in CMIP6 models

Olivia Ferguglia[1,3] · Jost von Hardenberg[2,3] · Elisa Palazzi[1,3]

Abstract

An Emergent Constraint (EC) is a physically-explainable relationship between model simulations of a past climate variable (predictor) and projections of a future climate variable (predictand). If a significant correlation exists between the predictand and the predictor, observations of the latter can be used to constrain model projections of the former and to narrow their uncertainties. In the present study, the EC technique has been applied to the analysis of precipitation, one of the variables most affected by model uncertainties and still insufficiently analysed in the context of ECs, particularly for the recent CMIP6 model ensemble. The main challenge in determining an EC is establishing if the relationship found is physically meaningful and robust to the composition of the model ensemble. Four precipitation ECs already documented in the literature and so far tested only with CMIP3/CMIP5, three of them involving the analysis of extreme precipitation, have been reconsidered in this paper. Their existence and robustness are evaluated using different subsets of CMIP5 and CMIP6 models, verifying if the EC is still present in the most recent ensemble and assessing its sensitivity to the detailed ensemble composition. Most ECs considered do not pass this test: we found one EC not to be robust in both CMIP5 and CMIP6, other two exist and are robust in CMIP5 but not in CMIP6, and only one is verified and is robust in both model ensembles.

Keywords Emergent Constraint · Climate model uncertainty · CMIP6 · Precipitation extremes

1 Introduction

Climate models are fundamental tools to understand the complexity of the Earth system and the processes at play, and to provide credible projections of future climate evolution. Unfortunately, models often disagree on the amplitude and sometimes on the sign of climate change signals. One source of uncertainty relies on the representation of processes that cannot be explicitly described because, e.g, they take place at scales smaller than the model resolution. These processes are included by means of parameterizations that can be different from model to model. Thus, the choice of one parameterization introduces, also through the triggering of numerous climate feedbacks, significant sources of model spread. A better understanding of model uncertainties and of their sources, and a reduction of the inter-model spread are essential steps in model development, evaluation and validation, with the aim of increasing the confidence in future projections.

In recent years, a methodology called "Emergent Constraints (ECs)", pioneered by Hall and Qu (2006), has been further developed and utilized as an approach for reducing uncertainties in climate change projections. An EC is a physically-explainable empirical relationship between inter-model variations in a quantity describing some aspects of the observed climate—the current climate predictor—and inter-model variations in a future prediction of some climate quantity—the future climate predictand (Klein and Hall 2015). The most important requirement for a trustworthy EC is that a strong physical explanation exists for the predictor-predictand correlation. A three-step definition has been proposed to establish an EC: (1) a *potential* EC is one in which a significant correlation exists between the predictor and the predictand; (2) a *promising* EC is when a physical explanation is proposed to support the correlation; and (3) an EC is *confirmed* if a strong physically-based evidence that justifies the correlation between the predictor and the predictand (i.e., the proposed explanation at item 2) is

✉ Olivia Ferguglia
  olivia.ferguglia@unito.it; o.ferguglia@isac.cnr.it

1 Department of Physics, University of Turin, Turin, Italy

2 Department of Environment, Land and Infrastructure Engineering, Politecnico di Torino, Turin, Italy

3 Institute of Atmospheric Science and Climate, National Research Council (ISAC-CNR), Turin, Italy

verified (Klein and Hall 2015). Recently, Hall et al. (2019) presented a framework whereby a *potential* EC is promoted to *confirmed* when the EC is accompanied by a plausible and explainable physical mechanism and assessing whether it survives out-of-sample testing (Simpson et al. 2021).

During the last decades, as the potential of the ECs as a technique to reduce the inter-model spread was recognised (Hall and Qu 2006), a number of ECs has been tested and applied in different branches of the climate science, including studies of Equilibrium Climate Sensitivity, cloud feedbacks, analyses of the carbon cycle and high-latitude processes, applications to the hydrological cycle and still others (e.g., Brient 2020; Williamson et al. 2021). Among them, applications to the water cycle and its different components—particularly precipitation—have not been so widely investigated.

Precipitation is one of the most difficult variables both to measure and to model, and it is a considerable source of uncertainty in climate model simulations (Trenberth and Zhang 2022; Chen et al. 2021; Na et al. 2020). In fact, many processes of precipitation formation are not explicitly resolved but described by means of parameterizations, so that the inter-model spread in the global-mean precipitation response to the temperature increase appears to be large in global warming simulations (Fläschner et al. 2016). All this suggests that precipitation is a crucial variable to develop ECs, with the aim of reducing uncertainties in model projections, also considering that precipitation changes have large impacts on natural and human systems. Nevertheless, a very limited number of precipitation ECs has been proposed and analysed to date (Borodina et al. 2017; O'Gorman 2012; Deangelis et al. 2015; Li et al. 2017; Watanabe et al. 2018; Rowell 2019; Thackeray et al. 2022).

Recently, Caldwell et al. (2018) and Hall et al. (2019) showed that a relevant number of hydrological cycle-related ECs analysed in the literature lack a satisfying physical explanation: owing to the large number of possible observables and the relatively small number of models, spurious relationships might result by chance (Caldwell and et al. 2014). Furthermore, most of the ECs recently published use models from only the Coupled Model Intercomparison Project phase 5 (CMIP5, Taylor et al. 2012) to test the statistical relationship between the predictor and the predictand. As suggested by Hall et al. (2019), to demonstrate the robustness of an EC, other model ensembles, and in particular the most recent CMIP6 (Eyring et al. 2016), should be used, a validation which, so far, has been performed only in a limited number of cases (Pendergrass 2020; Schlund et al. 2020; Simpson et al. 2021).

In the present paper, we reconsider four precipitation ECs which were originally identified using previous generations of model ensembles (CMIP3 and CMIP5, Meehl et al. 2007), and analyze to what extent they are still verified

in CMIP6—including a comparison with CMIP5, checking both their existence in the new ensemble and their robustness as suggested by Simpson et al. (2021). The majority of the ECs considered in this study do not pass this test, confirming that the identification of Emergent Constraint mechanisms for hydrological variables requires extensive validation and often does not survive in the latest generation of models.

This paper is structured as follows: in Sect. 2, the employed model data and methods applied in our analysis are described; results are presented in Sect. 3 for each of the four ECs, while Sect. 4 discusses and concludes the paper.

2 Model data and methods

2.1 Model data

The output of 27 global climate models (GCMs) from CMIP5 and of 29 GCMs from CMIP6 was analysed. The selected models are shown in Table 1. Data were downloaded from the Earth System Grid Federation (ESGF) with the Synda tool (https://portal.enes.org/data/data-metadata-service/data-discovery/synda). We selected the models for which daily precipitation and monthly temperature data were available at the time when we downloaded the data (May 2021). The requirement of daily precipitation data comes from the fact that this paper analyses ECs involving the calculation of precipitation extremes, as detailed in Sect. 2.2. In order to accomplish a fair comparison among the various models and between historical and future conditions, we considered only the models for which the same ensemble member was available both in the historical and in the scenario simulations.

Data were selected from the historical experiment of each model, to define a present climatology, and from scenario simulations (using RCP8.5 in CMIP5 and SSP585 in CMIP6, Meinshausen et al. 2011; Kriegler et al. 2017) to define a future climatology. The time period chosen to define either the past or future climatology was not necessarily the same for each EC, as better explained in the Supplementary Information and summarized in Table 2 (second and third column). The following model variables were considered: daily mean precipitation flux (pr), monthly near-surface air temperature (tas) and monthly surface temperature (ts).

2.2 General description of the chosen ECs and of their analysis methods

We recall that an EC is defined as a physically explainable relationship between a predictor and a predictand, as explained in Sect. 1. Throughout this paper, each EC is identified with an acronym whose last letter indicates the initial

Table 1 CMIP5 (left) and CMIP6 (right) models considered in this study, accompanied by a key reference

CMIP5			CMIP6		
Model name	Institution name	Reference	Model name	Institution name	Reference
ACCESS1-0	CSIRO-BOM	Bi et al. (2013)	ACCESS-ESM1-5	CSIRO	Tilo et al. (2020)
ACCESS1-3	CSIRO-BOM	Bi et al. (2013)	ACCESS-CM2	CSIRO-ARCCSS	Bi et al. (2013)
bcc-csm1-1	BCC	Wu et al. (2014)	BCC-CSM2-MR	BCC	Wu et al. (2021)
bcc-csm1-1-m	BCC	Wu et al. (2014)	CanESM5	CCCma	Swart et al. (2019)
CanESM2	CCCma	Arora et al. (2011)	CESM2	NCAR	Danabasoglu et al. (2020)
CCSM4	NCAR	Meehl et al. (2012)	CESM2-WACCM	NCAR	Gettelman et al. (2019)
CESM1-BGC	NSF-DOE-NCAR	Hurrell et al. (2013)	CMCC-CM2-SR5	CMCC	Cherchi et al. (2019)
CESM1-CAM5	NSF-DOE-NCAR	Hurrell et al. (2013)	CMCC-ESM2	CMCC	Cherchi et al. (2019)
CNRM-CM5	CNRM-CERFACS	Voldoire et al. (2013)	CNRM-CM6-1	CNRM	Voldoire et al. (2019)
CSIRO-Mk3-6-0	CSIRO-QCCCE	Rotstayn et al. (2012)	EC-Earth3	EC-Earth-Cons	Döscher et al. (2022)
FGOALS-g2	LASG-CESS	Li et al. (2013)	EC-Earth3-CC	EC-Earth Cons	Döscher et al. (2022)
GFDL-ESM2G	NOAA-GFDL	Delworth et al. (2006)	EC-Earth3-Veg	EC-Earth Cons	Döscher et al. (2022)
GFDL-ESM2M	NOAA-GFDL	Delworth et al. (2006)	EC-Earth3-Veg-LR	EC-Earth Cons	Döscher et al. (2022)
HadGEM2-CC	MOHC	Martin et al. (2011)	FGOALS-g3	CAS	Li et al. (2020)
HadGEM2-ES	MOHC	Bellouin et al. (2011)	GFDL-ESM4	NOAA-GFDL	Dunne et al. (2020)
INM-CM4	INM	Volodin et al. (2010)	GFDL-CM4	NOAA-GFDL	Adcroft et al. (2019)
IPSL-CM5A-LR	IPSL	Hourdin et al. (2013)	IITM-ESM	CCCR-IITM	Krishnan et al. (2019)
IPSL-CM5A-MR	IPSL	Hourdin et al. (2013)	INM-CM4-8	INM	Volodin et al. (2017)
IPSL-CM5B-LR	IPSL	Hourdin et al. (2013)	INM-CM5-0	INM	Volodin et al. (2017)
MIROC5	MIROC	Watanabe et al. (2010)	IPSL-CM6A-LR	IPSL	Boucher et al. (2020)
MIROC-ESM	MIROC	Watanabe et al. (2011)	KIOST-ESM	KIOST	Pak et al. (2021)
MIROC-ESM-CHEM	MIROC	Watanabe et al. (2011)	MIROC6	MIROC	Tatebe et al. (2019)
MPI-ESM-LR	MPI	Giorgetta et al. (2013)	MPI-ESM1-2-LR	MPI	Mauritsen et al. (2019)
MPI-ESM-MR	MPI	Giorgetta et al. (2013)	MPI-ESM1-2-HR	MPI	Müller et al. (2018)
MRI-CGCM3	MRI	Yukimoto et al. (2012)	MRI-ESM2-0	MRI	Yukimoto et al. (2019)
MRI-ESM1	MRI	Adachi et al. (2013)	NESM3	NUIST	Cao et al. (2018)
NorESM1-M	NCC	Bentsen et al. (2013)	NorESM2-LM	NCC	Seland et al. (2020)
			NorESM2-MM	NCC	Seland et al. (2020)
			TaiESM	AS-RCEC	Lee et al. (2020)

The ensemble member r1i1p1 was considered for CMIP5 and r1i1p1f1 for CMIP6

of the surname of the author that first proposed it. The first three columns of Table 2 list, for each EC, the variables taken as the predictor and predictand and the time periods over which they are evaluated (the last three columns summarize the results from the literature and from our study and will be discussed later). Here we provide a general overview of the four ECs considered in this study and describe the methods common to their analysis, while a more specific explanation of each EC and of the corresponding analysis methods is provided in the Supplementary Information.

- ECT (from Thackeray et al. 2018) assesses a relationship between global-mean hydrological sensitivity and local changes in extreme precipitation. The global-mean hydrological sensitivity (global-mean HS, the predictor) is defined as the global-mean precipitation change normalized by global-mean surface air temperature change.

The predictand is calculated as the change of the 99th percentile of precipitation, normalized by the global-mean surface air temperature change ($\Delta P_{99}/\Delta T$). Changes are evaluated as the difference between the 2060–2099 future climatology and the 1960–1999 past climatology. Even though the predictor contains information on the future climate and, as such, does not satisfy the proper definition of an EC, we decided to consider also the relationship analysed by Thackeray et al. (2018) in the context of Emergent Constraints.

- ECL (from Li et al. 2017) establishes a relationship between western Pacific precipitation and the change in Indian Summer Monsoon rainfall. The predictor is the past time- and space-mean daily precipitation in a western Pacific region (140°–190°W and 12°S–12°N, WP precipitation) while the predictand is represented by the future change of mean daily precipitation averaged over

Table 2 Summary of the ECs reconsidered in this study

Acronym	Predictor	Predictand	Original result	CMIP5	CMIP6
ECT	Global-mean HS ($\%K^{-1}$) 1960–1999	$\Delta P_{99}/\Delta T$ (mm/year K^{-1}) 2060–2099	r≥0.6 in oceanic tropical regions (CMIP5)	r≥0.6 with p<0.05 in oceanic tropical regions	r≥0.6 with p<0.05 in southern tropical Indian ocean
ECL	WP precipitation (mm/day) 1980–2009	ISM rainfall change (mm/day $°C^{-1}$) 2070–2099	r = 0.63 (CMIP5)	r = 0.56 $p = 2 \times 10^{-3}$	r = 0.03 p = 0.89
ECG	Sensitivity for variability ($\%K^{-1}$) 1981–1999	Sensitivity for climate change ($\%K^{-1}$) 2081–2099	r = 0.87 (CMIP3)	r = 0.75 $p = 8 \times 10^{-6}$	r = 0.73 $p = 7 \times 10^{-6}$
ECB	Rx1day scaling historical ($\%K^{-1}$) 1951–2014	Rx1day scaling future 8.5 ($\%K^{-1}$) 2015–2099	r = 0.82 (CMIP5)	r = 0.88 $p = 2 \times 10^{-9}$	r = 0.38 p = 0.04

The first four columns show, respectively, the EC acronym, the predictor and predictand definitions along with their reference periods, and the results discussed in the original papers in terms of correlation coefficients (all being statistically significant). The last two columns show our results (correlation coefficient, r, and p-value) obtained with CMIP5 and CMIP6 models

the region 60°–95°E, 10°–30°N during the Indian Summer Monsoon season (May to September) normalized by global-mean SST change (ISM rainfall change). In this case, the future change is evaluated as the difference between the 2070–2099 future climatology and the 1980–2009 past climatology.

- ECG (from O'Gorman 2012) defines a relationship between extreme tropical precipitation (99.9th percentile) scaled with surface air temperature over tropical oceans during the past reference period 1981–1999 (this quantity is referred to as "Sensitivity for variability", as in the original paper), and the future change in tropical extreme precipitation divided by temperature increase over the Tropics (called "Sensitivity for climate change"). In this context, the scaling procedure consists in calculating the slope between monthly time series of extreme precipitation and surface air temperature over the tropical ocean, then normalized by time- (1981–1999) and space- (the Tropics, between 30°S–30°N) averaged extreme precipitation. The future change is evaluated as the difference between the 2081–2099 future climatology and the 1981–1999 past climatology. Fur further details on the scaling procedure, please refer to O'Gorman (2012).

- ECB (from Borodina et al. 2017) correlates the annual maximum value of daily precipitation amounts (Rx1day index, Karl et al. 1999) scaled with global-land temperature (Rx1day scaling), calculated over a past time period (1951–2014), to the same quantity calculated over a future period (2015–2099) in different regions of the world characterized by high climatological rainfall intensity. The scaling method in this case requires the

calculation of the Theil-Sen slope (von Storch and Zwiers 1984) of the relationship between the yearly time series of Rx1day and mean surface air temperature, then normalized by space- and time-averaged Rx1day index. For the definition of the predictand, we chose the period 2015–2099 instead of 1951–2099 used by Borodina et al. (2017) in order not to include the window 1951–2014 over which the predictor is defined.

For each EC, a preliminary analysis has been performed to reproduce the results found in the reference papers using the same (or a very similar) set of models (from CMIP5) employed by the original authors (Thackeray et al. 2018; Li et al. 2017; Borodina et al. 2017). This analysis produced successful results for each EC and will not be discussed in subsequent sections. Then, each EC was tested with the CMIP5 and CMIP6 model ensembles selected for this study (see Table 1). A bootstrap analysis was performed for both model ensembles, taking random sub-samples of about 2/3 of the complete model set (where not differently specified) and repeating this procedure 10000 times, to reproduce the predictor-predictand relationship. The distribution of the correlation coefficients describing the EC was analysed to check for the EC robustness.

3 Results

In this section, we present the results of our analysis applied to the four ECs taken into consideration—a summary of the results is provided in the three rightmost columns of Table 2.

3.1 ECT

Figures 1(a, b) show, for CMIP5 and CMIP6 respectively, the spatial map of the inter-model correlation between global-mean HS (% K^{-1}) and local changes in extreme precipitation ($\Delta P_{99}/\Delta T$ (mm/year K^{-1})), respectively the predictor and the predictand in this EC. Dotted areas indicate where the correlation exceeds the 95% significance level (p ≤ 0.05).

Figure 1a, referring to CMIP5, shows that the areas with significant correlation are found around the Tropics, especially in the Pacific ocean, in the western Atlantic and coastal areas of Venezuela and Brazil, in the Indian ocean, and in Indonesia, in agreement with the results found by Thackeray et al. (2018).

The same analysis performed with CMIP6 models is presented in panel b: in the Tropics, the correlation coefficient decreases considerably in all regions outlined above except in a small area in the Indian Ocean and around Indonesia, where r ≥ 0.6. To better explore the reasons for this different behaviour in the two model ensembles, the inter-model standard deviation of the predictand for CMIP5 and CMIP6 models has been evaluated and is shown in Fig. 1(panels c and d, respectively). CMIP6 models agree better with each

other (smaller standard deviation) than CMIP5 models in projecting local extreme precipitation. On the other hand, global-mean HS does not change between CMIP5 (ensemble mean equal to 0.047 ± 0.008 %K^{-1}) and CMIP6 (0.046 ± 0.009 %K^{-1}). Our interpretation is that the reduced CMIP6 inter-model spread in the predictand prevents this relationship from still working as an EC, since the variability associated with a possible influence of the predictor can be smaller than the natural sample variability in the predictand.

3.2 ECL

Figure 2 shows the scatterplot between the predictor (mean western Pacific precipitation, (mm/day)) and the predictand (future change of ISM precipitation, (mm/day °C^{-1})) calculated with CMIP5 (panel a) and CMIP6 (panel b) models. Figure 2a shows that the two variables are positively correlated with a correlation coefficient of 0.56, not dissimilar to the one found by Li et al. (2017), (i.e. 0.63, in Fig. 2a of their original paper). For this specific EC, in order to check the sensitivity of the results to the ensemble composition, we performed a bootstrap test using a 27 sub-sample of a larger set of CMIP5 models (39 models overall, the extra ones from our set are
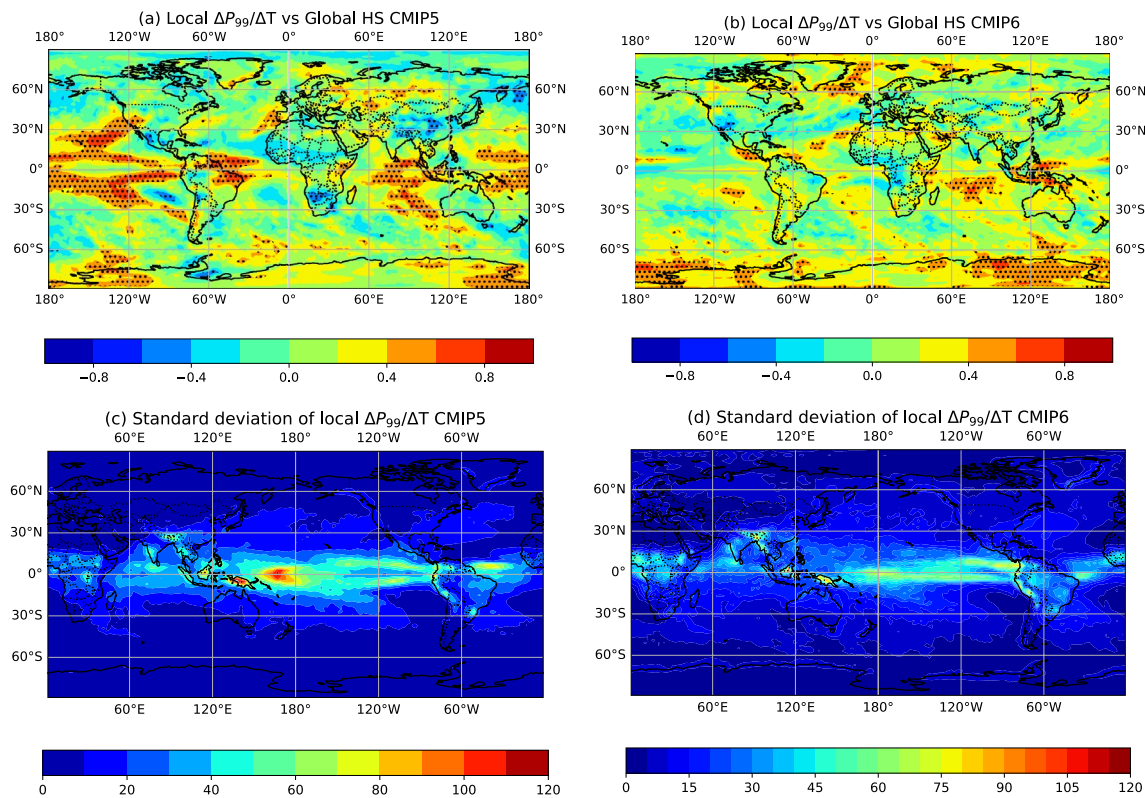

Fig. 1 Analysis of ECT. **a** Inter-model correlation between the predictor (global-mean HS—(% K^{-1})) and the predictand (local change in extreme precipitation per degree of global warming—(mm/year K^{-1})) for CMIP5. Dotted areas show statistically-significant correlations (p ≤ 0.05). **b** Same as **a** but for CMIP6. **c**, **d** Inter-model standard deviation of the predictand for CMIP5 (**c**) and CMIP6 (**d**)
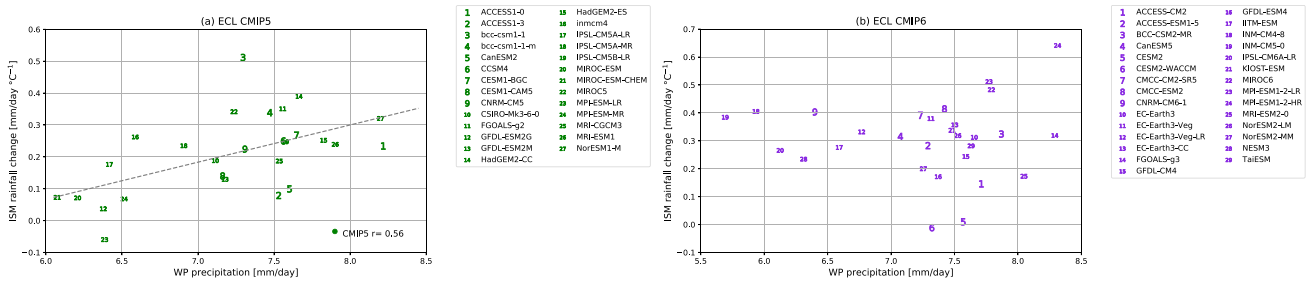
Fig. 2 Analysis of ECL. **a** Scatterplot of the predictand (future change of ISM precipitation—(mm/day °C^{-1})) against the predictor (western Pacific precipitation—(mm/day)) for CMIP5. The dashed line shows the ordinary least-squares best fit. **b** Same as **a** for CMIP6. Here the best-fit line is not shown as no significant correlation was found

reported in the Supplementary Information). These 39 models are those for which precipitation data at monthly resolution were available—this specific EC in fact does not require daily precipitation data for its calculation, thus monthly precipitation data, available for a larger number of models, can be used to increase the size of our ensemble. This bootstrap analysis led to an even lower mean correlation coefficient compared to the previous value (0.35 ± 0.10, against 0.56) which indicates that the correlation that supports this EC largely depends on the model ensemble composition. Thus, this EC may not be particularly robust whenever the goal is to use it to reduce uncertainties in model projections. The corresponding coefficient of variation (CV), the ratio of the standard deviation to the mean, is around 29% denoting a quite high variability of the correlation coefficient as a function of the specific composition of the ensemble. The probability distribution of the correlation coefficient is shown in the Supplementary Information (Figure S1).

The next step was to test the EC using CMIP6 models, as shown in panel b: in this case we found a correlation which drops dramatically to r = 0.03 (p value not significant), confirming that this EC does not survive changes in the model ensemble and in its composition.

3.3 ECG

Figure 3 shows the scatterplot between the predictor (sensitivity for variability, see Sect. 2.2) and the predictand (sensitivity for climate change) for both CMIP5 (panel a) and CMIP6 (panel b) models. Models in the CMIP5 ensemble with high sensitivity for variability tend to project a larger increase in sensitivity for climate change, with an inter-model correlation of 0.75 ($p \leq 0.05$, see Table 2). In this case, since there are no more available models for both CMIP5 and CMIP6 than those specified in Table 1 providing daily precipitation data required to calculate ECG, we performed a bootstrap analysis as described in Sect. 2.2, i.e., with sub-sets containing 2/3 of the models. This analysis produced a distribution of the correlation coefficients with a standard deviation of 0.08 (mean value of 0.75). Similar results are found for CMIP6 models (panel b), with a correlation coefficient of 0.73 ($p \leq 0.05$, 0.73 ± 0.07 from the bootstrap analysis). In both CMIP5 and CMIP6 cases, the coefficient of variation, CV, is relatively low, 11% in CMIP5 and 9.6% in CMIP6, showing a low dispersion of the correlation coefficients obtained from bootstrap analysis with respect to their mean (the probability distribution is shown in Figure S2 of the Supplementary Information). This analysis suggests that this EC exists in both CMIP5 and CMIP6 and that it is characterised by a high and significant correlation
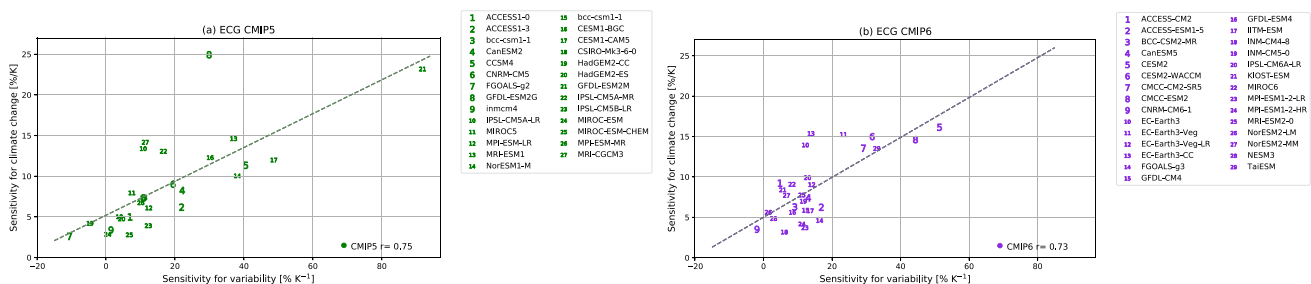

Fig. 3 Analysis of ECG. **a** Scatterplot of the predictand (sensitivity for climate change)—(% K^{-1})) against the predictor (sensitivity for variability—(% K^{-1})) for CMIP5. The dashed line shows the ordinary least-squares best fit. **b** Same as **a** but for CMIP6

coefficient between the predictor and the predictand. To further test this EC robustness we replicated the previous analysis using the SSP245 CMIP6 emission scenario. The results are consistent with those found for SSP585, resulting in a correlation coefficient of 0.85 ($p \leq 0.05$; $r = 0.84 \pm 0.07$ from the bootstrap analysis), which provides evidence of the ECG robustness. Figure S3 of the Supplementary Information shows the results of the analyses performed with the SSP245 scenario.

3.4 ECB

Figure 4 shows the scatterplot between the historical Rx1day scaling ($\%K^{-1}$) (the predictor) and future projections of the same quantity (the predictand) with both CMIP5 (Fig. 4a) and CMIP6 (Fig. 4b). As can be seen in panel a,

the correlation coefficient between the predictor and the predictand is high (0.88, $p \leq 0.05$) and similar to the one found by Borodina et al. (2017) in the original paper ($r = 0.82$). The bootstrap analysis performed on our CMIP5 ensemble led to an average correlation coefficient of 0.87 ± 0.04 and a CV of 5% (the probability distribution of r is shown in Figure S4 of the Supplementary Information), confirming the robustness of this relationship using CMIP5. Figure 4b presents the scatterplot computed with CMIP6 models: the correlation coefficient decreases as far as 0.38, with a p-value of 0.04. The bootstrap analysis led to a correlation coefficient probability distribution characterized by a standard deviation of 0.09 (mean value 0.38) and a CV of 24% (see Figure S4 of the Supplementary Information). In order to better understand the decrease of the correlation in CMIP6, global maps of inter-model standard deviation of the predictor and
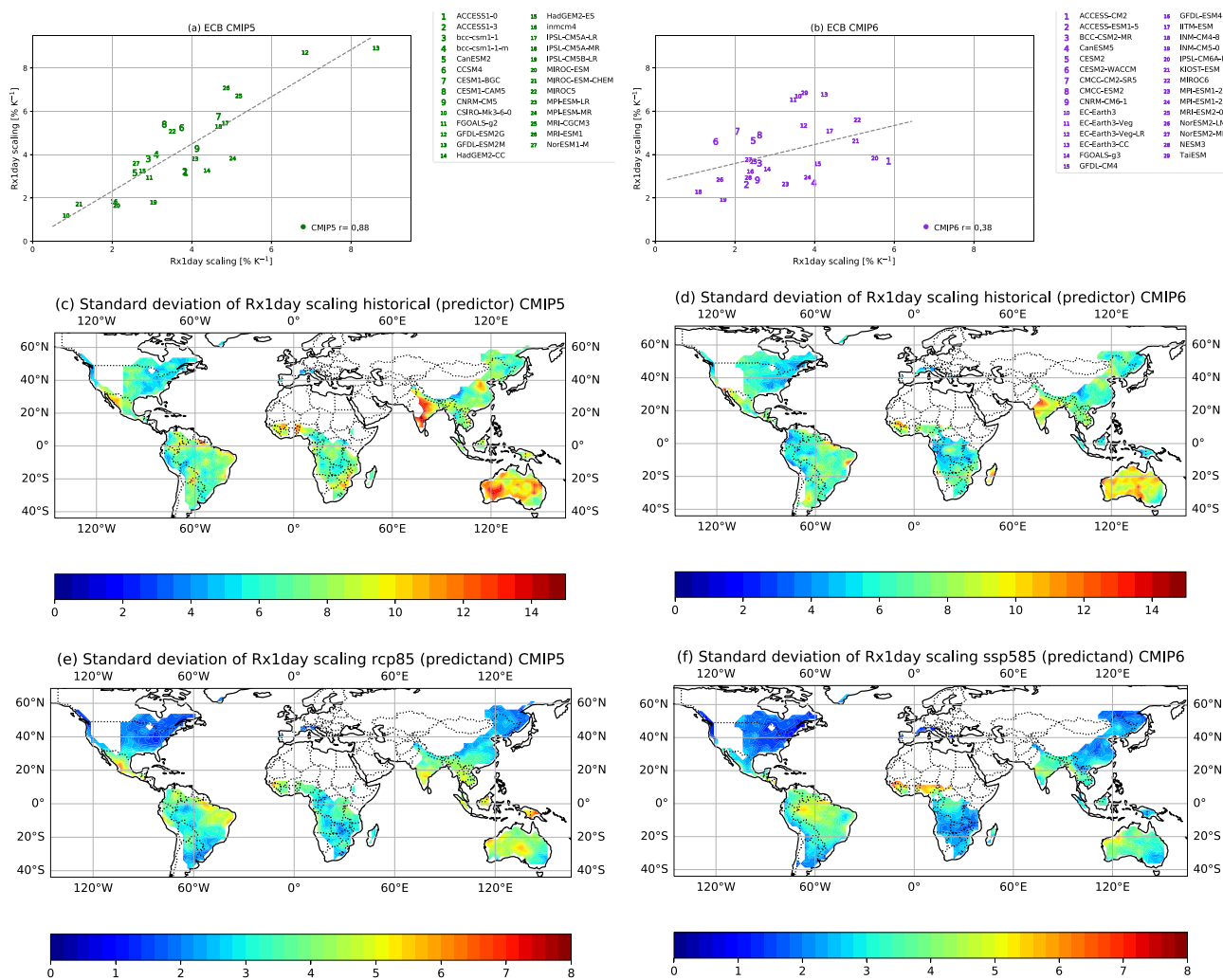

Fig. 4 Analysis of ECB. **a** Scatterplot of the predictand (Rx1day scaling—($\%~K^{-1}$)) against the predictor (Rx1day scaling—($\%~K^{-1}$)) for CMIP5. The dashed line shows the ordinary least-squares best fit. **b** Same as **a** but for CMIP6. **c**, **d** Intermodel standard deviation of the predictor for CMIP5, CMIP6. **e**, **f** Intermodel standard deviation of the predictand (Rx1day scaling—($\%~K^{-1}$)) for CMIP5, CMIP6

the predictand, for both CMIP5 and CMIP6, were calculated (see panels c–f of Fig. 4). For both the predictor and the predictand, the inter-model spread has clearly decreased in CMIP6 (panels d and f) with respect to CMIP5 (panels c and e). In particular, the regions showing the strongest reduction of the inter-model spread are India (for the predictor) and Africa and Southeast Asia (for the predictand). We provide further details computing spatial maps of the inter-model correlation between the predictor and the predictand (Figure S5 in the Supplementary Information). They highlight the regions that most contribute to the decrease of the correlation coefficient describing ECB, namely India, Africa and Southeast Asia, consistently with the previous finding. We hypothesize that spatial averaging performed over such diverse regions—inherent in the definition of this EC—may play a role in the decrease of the correlation in CMIP6. More generally, a reduction of the model uncertainty/spread in CMIP6 likely makes the application of this EC unnecessary to the aim of narrowing CMIP6 model projections.

4 Discussion and conclusions

In our analysis, we have reconsidered the existence and the strength of four precipitation ECs already proposed in the literature and we have tested their sensitivity to the ensemble composition using different CMIP5 and CMIP6 model ensembles. Our analysis suggests that only one EC (ECG) is robust with both CMIP5 and CMIP6 models, another one (ECL) is not robust with either CMIP5 or CMIP6 and the two remaining ones (ECT and ECB) are robust with CMIP5 but not with CMIP6.

ECG analyses the relationship between tropical extreme precipitation (scaled with temperature increase over tropical oceans) during the past (a quantity which O'Gorman (2012) called Sensitivity for variability) and tropical extreme precipitation (difference between a future and a past climatology) divided by temperature increase over the Tropics (called Sensitivity for climate change). As also suggested by O'Gorman (2012), who tested this EC in the CMIP3 ensemble, the strength of ECG arises from the fact that the predictor and the predictand are associated with the same physical process involved in precipitation formation (i.e. moist convection in the Tropics) which is included in the models by means of parameterizations. In the models, the latter are associated with similar inter-model spread in the response of tropical precipitation both in historical simulations (used to calculate the predictor) and in future projections (used to calculate the predictand). The sensitivity of ECG in CMIP6 was successfully tested not only for changes in the ensemble composition but also in different emission scenario, using both SSP245 and SSP585.

ECL establishes a relationship between western Pacific precipitation and the change in Indian Summer Monsoon rainfall, normalized by SST change. The physical process identified by the authors for this EC is related to the negative cloud-radiation feedback on sea surface temperatures: the negative feedback suppresses the local SST warming in the western Pacific area, strengthening ISM rainfall projections via atmospheric circulation. Our analysis does not lead to the same results as found in Li et al. (2017) since we found a very low correlation both in CMIP5 and in CMIP6. In addition to the described ECL analysis, an attempt to find a relevant correlation between the simulated tropical western Pacific precipitation and projected changes in SST warming patterns in the same area was done using CMIP6 models but no relevant correlation was found (r = − 0.04 with a p-value = 0.85). This result suggests that the proposed atmospheric mechanism responsible for the relationship between the predictor and the predictand should be better and deeply investigated in climate models. For example, the study by Palazzi et al. (2014), analyzing precipitation patterns and climatologies in the Indian monsoon region in CMIP5, showed that GCMs including the indirect effect of atmospheric aerosol reproduce better the climatology of Indian monsoon precipitation than the models including the direct effect of aerosol particles only. The same was found for the models incorporating a fully-interactive aerosol module than those with prescribed aerosols. This suggests that aerosol particles and their interactions with clouds could be important factors to be considered in the relationship found by Li et al. (2017) and, together with other factors, could be taken under consideration for further analyses trying to better understand the links between the variables involved in this EC. As discussed in the Introduction, several ECs were recently found to lack a satisfying physical basis able to sustain the correlation between the predictor and the predictand, and ECL may partially be ascribable to this category. The variables involved in this EC are probably too complex and a simple linear relationship that manages to both describe the EC and be used to narrow the model outputs can not be easily assessed.

ECT describes a relationship between global-mean precipitation change normalized by global-mean surface air temperature change and local changes in extreme precipitation. The physical mechanism behind this EC involves the relationship between the intensification of global hydrological cycle induced by global warming, changes in the atmospheric energy budget and increases in precipitation extremes. ECB correlates the annual maximum value of daily precipitation amounts scaled with global-land temperature increase in a past period to the same quantity calculated over a future period in different regions of the world characterized by high climatological rainfall intensity. Similarly to ECG, the formulation of this EC is based on the use of the

same variable for the predictor (evaluated in a past period) and the predictand (evaluated in the future) and thus the relationship that underlies the EC is somewhat straightforward. In addition, there is no difference in the ability of the models to simulate the same variable in the past and in the future as the equations and parameterizations describing it are the same.

In our analysis, both ECT and ECB turned out to be robust with CMIP5—thus in agreement with the reference literature—but not with CMIP6. We hypothesize that this could be attributed to a reduction of the model uncertainty in the CMIP6 ensemble with respect to CMIP5, which does not make the application of these Emergent Constraints effective. In particular, we found that the inter-model spread in the projections of extreme precipitation (99th percentile for ECT, Rx1day for ECB) is considerably narrowed in the latest generation of climate models. For this, an EC or, more generally, a relationship between two precipitation-related variables found with CMIP5 models may not be robust or even exist in CMIP6. While the inter-model spread in CMIP6 is reduced compared to CMIP5, it is still large and still needs to be reduced in order to produce future projections useful for climate-change adaptation strategies.

A new precipitation EC assessed by Thackeray et al. (2022) constrains future changes in the occurrence of extreme precipitation with historical simulations of the same variable. As already noticed from our analysis, it seems considerably more favorable to use the same variable for the predictor and the predictand, or at least variables that are regulated in the models by means of the same parameterizations and which can be ascribed to the same physical mechanisms. This observation helps to explain why ECG is the only EC which survives in the CMIP6 ensemble— and the new study by Thackeray et al. (2022) corroborates this hypothesis. One might then wonder why ECB does not behave in the same way as ECG, given that both use the same variable in the past and in the future as the predictor and the predictand, respectively. One possible explanation was provided in Sect. 3.4 and we believe that it lies in the spatial aggregation inherent in the ECB definition. In fact, ECB correlates extreme precipitation in the past and in the future averaged in different regions of the world, characterized by climatological high rainfall intensity. The aggregated areas are very different to each other, since they belong to different latitudinal zones and they are subjected to different climatological regimes. Precipitation is then associated with diverse large-scale and local mechanisms and all this could affect the overall model performance in the past and in the future. In fact, we found considerable geographical differences in the inter-model spread in both the predictor and the predictand (Fig. 4 panels c–f) as well as in their correlation maps (Fig. S5 in the Supplementary Information).

This also suggests that current ECs may be limited in their geographic applicability.

Another important consideration is that the Equilibrium Climate Sensitivity (ECS) has been proven to exhibit substantial differences between CMIP5 and CMIP6, both in the mean value and in the inter-model variability (Zelinka et al. 2020). We considered the possibility that this difference, especially in the inter-model spread, may play a role in the robustness of ECs (in particular of ECT and ECB which show the major differences between the CMIP5 and CMIP6 ensembles). We think that the higher inter-model spread in ECS (in CMIP6) may introduce an additional source of uncertainty, thus reducing the signal (the correlation behind the ECs) to noise ratio. Besides influencing its robustness, the introduction of such an uncertainty makes it even more difficult to effectively use the EC technique to constrain model uncertainties in projections.

Precipitation ECs are very powerful tools for understanding and investigating climate model response to mechanisms and dynamics linked to precipitation formation, trends and evolution. However, the analysis shown here suggests that their practical application for reducing uncertainties in model projections linking them to observable metrics should be regarded with caution, due to the large sensitivity of the EC to the model ensemble composition, which represents a weakness of the technique. In conclusion, as also suggested by Sanderson et al. (2021), the strength and potential of the EC technique should be mostly linked to its capability to interpret climate phenomena and to describe and investigate the connections between different climate variables—thus improving our knowledge of the climate system and its mechanisms, rather than (only) to its power to effectively narrow uncertainties in climate change projections. Exploring new emergent constraints and using them in new model ensembles thus represent a valuable way first and foremost to improve simulations of current climate and to better understand climate dynamics.

Code and data availability Available on request.

Declarations

Conflict of interest The authors declare that they have no relevant financial or non-financial interests to disclose.

Ethical approval Not applicable.

References

Adachi Y, Yukimoto S et al (2013) Basic performance of a new earth system model of the meteorological research institute. Pap Meteorol Geophys 64:25. https://doi.org/10.2467/mripapers.64.1

Adcroft A, Anderson W et al (2019) The GFDL global ocean and sea ice model OM4.0: model description and simulation features. J Adv Model Earth Syst 11:20. https://doi.org/10.1029/2019MS001726

Arora VK, Scinocca JF et al (2011) Carbon emission limits required to satisfy future representative concentration pathways of greenhouse gases. Geophys Res Lett. https://doi.org/10.1029/2010GL046270

Bellouin N, Rae J, Jones A, Johnson C, Haywood J, Boucher O (2011) Aerosol forcing in the climate model intercomparison project (CMIP5) simulations by HADGEM2-ES and the role of ammonium nitrate. J Geophys Res Atmos. https://doi.org/10.1029/2011JD016074

Bentsen M, Bethke I et al (2013) The Norwegian earth system model, NORESM1-M-part 1: description and basic evaluation of the physical climate. Geosci Model Dev. https://doi.org/10.5194/gmd-6-687-2013

Bi D, Dix M et al (2013) The access coupled model: description, control climate and evaluation. Aust Meteorol Oceanogr J. https://doi.org/10.22499/2.6301.004

Borodina A, Fischer EM, Knutti R (2017) Emergent constraints in climate projections: a case study of changes in high-latitude temperature variability. J Clim. https://doi.org/10.1175/JCLI-D-16-0662.1

Boucher O, Servonnat J et al (2020) Presentation and evaluation of the IPSL-CM6A-LR climate model. J Adv Model Earth Syst. https://doi.org/10.1029/2019MS002010

Brient F (2020) Reducing uncertainties in climate projections with emergent constraints: concepts, examples and prospects. Adv Atmos Sci. https://doi.org/10.1007/s00376-019-9140-8

Caldwell PM et al (2014) Statistical significance of climate sensitivity predictors obtained by data mining. Geophys Res Lett. https://doi.org/10.1002/2014GL059205

Caldwell PM, Zelinka MD, Klein SA (2018) Evaluating emergent constraints on equilibrium climate sensitivity. J Clim. https://doi.org/10.1175/JCLI-D-17-0631.1

Cao J, Wang B et al (2018) The Nuist earth system model (NESM) version 3: description and preliminary evaluation. Geosci Model Dev. https://doi.org/10.5194/gmd-11-2975-2018

Chen D, Dai A, Hall A (2021) The convective-to-total precipitation ratio and the "drizzling'' bias in climate models. J Geophys Res Atmos. https://doi.org/10.1029/2020JD034198

Cherchi A, Fogli PG et al (2019) Global mean climate and main patterns of variability in the CMCC-CM2 coupled model. J Adv Model Earth Syst. https://doi.org/10.1029/2018MS001369

Danabasoglu G, Lamarque JF et al (2020) The community earth system model version 2 (CESM2). J Adv Model Earth Syst. https://doi.org/10.1029/2019MS001916

Deangelis AM, Qu X, Zelinka MD, Hall A (2015) An observational radiative constraint on hydrologic cycle intensification. Nature. https://doi.org/10.1038/nature15770

Delworth TL, Broccoli AJ et al (2006) Gfdl's cm2 global coupled climate models. Part I: formulation and simulation characteristics. J Clim. https://doi.org/10.1175/JCLI3629.1

Döscher R, Acosta M, Alessandri A (2022) The EC-Earth3 Earth system model for the Coupled Model Intercomparison Project 6. Geosci Model Dev 15(7):2973–3020. https://gmd.copernicus.org/articles/15/2973/2022/

Dunne JP, Horowitz LW et al (2020) The GFDL earth system model version 4.1 (GFDL-ESM 4.1): overall coupled model description and simulation characteristics. J Adv Model Earth Syst. https://doi.org/10.1029/2019MS002015

Eyring V, Bony S et al (2016) Overview of the coupled model intercomparison project phase 6 (CMIP6) experimental design and organization. Geosci Model Dev. https://doi.org/10.5194/gmd-9-1937-2016

Fläschner D, Mauritsen T, Stevens B (2016) Understanding the intermodel spread in global-mean hydrological sensitivity. J Clim 29:151118151605004. https://doi.org/10.1175/JCLI-D-15-0351.1

Gettelman A, Hannay C et al (2019) High climate sensitivity in the community earth system model version 2 (CESM2). Geophys Res Lett. https://doi.org/10.1029/2019GL083978

Giorgetta MA, Jungclaus J et al (2013) Climate and carbon cycle changes from 1850 to 2100 in MPI-ESM simulations for the coupled model intercomparison project phase 5. J Adv Model Earth Syst. https://doi.org/10.1002/jame.20038

Hall A, Qu X (2006) Using the current seasonal cycle to constrain snow albedo feedback in future climate change. Geophys Res Lett. https://doi.org/10.1029/2005GL025127

Hall A, Cox P, Huntingford C, Klein S (2019) Progressing emergent constraints on future climate change. Nat Clim Change. https://doi.org/10.1038/s41558-019-0436-6

Hourdin F, Foujols MA et al (2013) Impact of the LMDZ atmospheric grid configuration on the climate and sensitivity of the IPSL-CM5A coupled model. Clim Dyn. https://doi.org/10.1007/s00382-012-1411-3

Hurrell JW, Holland MM et al (2013) The community earth system model: a framework for collaborative research. Bull Am Meteorol Soc. https://doi.org/10.1175/BAMS-D-12-00121.1

Karl TR, Nicholls N, Ghazi A (1999) Clivar/gcos/wmo workshop on indices and indicators for climate extremes—workshop summary. Clim Change. https://doi.org/10.1023/A:1005491526870

Klein SA, Hall A (2015) Emergent constraints for cloud feedbacks. Curr Clim Change Rep. https://doi.org/10.1007/s40641-015-0027-1

Kriegler E, Bauer N et al (2017) Fossil-fueled development (SSP5): an energy and resource intensive scenario for the 21st century. Glob Environ Change. https://doi.org/10.1016/j.gloenvcha.2016.05.015

Krishnan R, Swapna P, et al (2019) Current trends in the representation of physical processes in weather and climate models. Springer Singapore, Singapore, chap The IITM Earth System Model (ESM): development and future roadmap, pp 183–195. https://doi.org/10.1007/978-981-13-3396-5_9

Lee WL, Wang YC et al (2020) Taiwan earth system model version 1: description and evaluation of mean state. Geosci Model Dev. https://doi.org/10.5194/gmd-13-3887-2020

Li L, Lin P et al (2013) The flexible global ocean-atmosphere-land system model, grid-point version 2: Fgoals-g2. Adv Atmos Sci. https://doi.org/10.1007/s00376-012-2140-6

Li L, Yu Y et al (2020) The flexible global ocean-atmosphere-land system model grid-point version 3 (FGOALS-G3): description and evaluation. J Adv Model Earth Syst. https://doi.org/10.1029/2019MS002012

Li G, Xie SP, He C, Chen Z (2017) Western pacific emergent constraint lowers projected increase in Indian summer monsoon rainfall. Nat Clim Change. https://doi.org/10.1038/nclimate3387

Martin GM, Bellouin N et al (2011) The HADGEM2 family of met office unified model climate configurations. Geosci Model Dev. https://doi.org/10.5194/gmd-4-723-2011

Mauritsen T, Bader J et al (2019) Developments in the MPI-M earth system model version 1.2 (MPI-ESM1.2) and its response to increasing co2. J Adv Model Earth Syst. https://doi.org/10.1029/2018MS001400

Meehl GA, Covey C et al (2007) The WCRP CMIP3 multimodel dataset: a new era in climatic change research. Bull Am Meteorol Soc. https://doi.org/10.1175/BAMS-88-9-1383

Meehl GA, Washington WM et al (2012) Climate system response to external forcings and climate change projections in ccsm4. J Clim. https://doi.org/10.1175/JCLI-D-11-00240.1

Meinshausen M, Smith SJ et al (2011) The RCP greenhouse gas concentrations and their extensions from 1765 to 2300. Clim Change. https://doi.org/10.1007/s10584-011-0156-z

Müller WA, Jungclaus JH et al (2018) A higher-resolution version of the max Planck institute earth system model (MPI-ESM1.2-HR). J Adv Model Earth Syst. https://doi.org/10.1029/2017MS001217

Na Y, Fu Q, Kodama C (2020) Precipitation probability and its future changes from a global cloud-resolving model and cmip6 simulations. J Geophys Res Atmos. https://doi.org/10.1029/2019JD031926

O'Gorman PA (2012) Sensitivity of tropical precipitation extremes to climate change. Nat Geosci. https://doi.org/10.1038/ngeo1568

Pak G, Noh Y et al (2021) Korea institute of ocean science and technology earth system model and its simulation characteristics. Ocean Sci J. https://doi.org/10.1007/s12601-021-00001-7

Palazzi E, von Hardenberg J, Sea T (2014) Precipitation in the Karakoram-Himalaya: a CMIP5 view. Clim Dyn. https://doi.org/10.1007/s00382-014-2341-z

Pendergrass AG (2020) The global-mean precipitation response to co2-induced warming in cmip6 models. Geophys Res Lett. https://doi.org/10.1029/2020GL089964

Rotstayn LD, Jeffrey SJ et al (2012) Aerosol- and greenhouse gas-induced changes in summer rainfall and circulation in the Australasian region: a study using single-forcing climate simulations. Atmos Chem Phys. https://doi.org/10.5194/acp-12-6377-2012

Rowell DP (2019) An observational constraint on cmip5 projections of the east African long rains and southern Indian ocean warming. Geophys Res Lett. https://doi.org/10.1029/2019GL082847

Sanderson BM, Pendergrass AG et al (2021) The potential for structural errors in emergent constraints. Earth Syst Dyn. https://doi.org/10.5194/esd-12-899-2021

Schlund M, Lauer A, Gentine P, Sherwood SC, Eyring V (2020) Emergent constraints on equilibrium climate sensitivity in CMIP5: do they hold for CMIP6? Earth Syst Dyn. https://doi.org/10.5194/esd-11-1233-2020

Seland Ø, Bentsen M, Olivié D (2020) Overview of the Norwegian earth system model (NORESM2) and key climate response of cmip6 deck, historical, and scenario simulations. Geosci Model Dev 13(12):6165–6200. https://gmd.copernicus.org/articles/13/6165/2020/

Simpson IR, McKinnon KA et al (2021) Emergent constraints on the large-scale atmospheric circulation and regional hydroclimate: do they still work in cmip6 and how much can they actually constrain the future? J Clim. https://doi.org/10.1175/JCLI-D-21-0055.1

Swart NC, Cole JN et al (2019) The Canadian earth system model version 5 (canesm5.0.3). Geosci Model Dev. https://doi.org/10.5194/gmd-12-4823-2019

Tatebe H, Ogura T et al (2019) Description and basic evaluation of simulated mean state, internal variability, and climate sensitivity in miroc6. Geosci Model Dev. https://doi.org/10.5194/gmd-12-2727-2019

Taylor KE, Stouffer RJ, Meehl GA (2012) An overview of CMIP5 and the experiment design. Bull Am Meteorol Soc. https://doi.org/10.1175/BAMS-D-11-00094.1

Thackeray CW, DeAngelis AM, Hall A, Swain DL, Qu X (2018) On the connection between global hydrologic sensitivity and regional wet extremes. Geophys Res Lett. https://doi.org/10.1029/2018GL079698

Thackeray CW, Hall A, Norris J, Chen D (2022) Constraining the increased frequency of global precipitation extremes under warming. Nat Clim Change 12:441–448. https://doi.org/10.1038/s41558-022-01329-1

Trenberth KE, Zhang Y (2022) How often does it really rain? Bull Am Meteorol Soc 99(2):289–298. https://doi.org/10.1175/BAMS-D-17-0107.1

Voldoire A, Sanchez-Gomez E, Mélia DS et al (2013) The CNRM-CM5.1 global climate model: description and basic evaluation. Clim Dyn. https://doi.org/10.1007/s00382-011-1259-y

Voldoire A, Saint-Martin D, et al (2019) Evaluation of CMIP6 deck experiments with CNRM-CM6-1. J Adv Model Earth Syst. https://doi.org/10.1029/2019MS001683

Volodin EM, Mortikov EV et al (2017) Simulation of the present-day climate with the climate model inmcm5. Clim Dyn. https://doi.org/10.1007/s00382-017-3539-7

Volodin EM, Dianskii NA, Gusev AV (2010) Simulating present-day climate with the INMCM4.0 coupled model of the atmospheric and oceanic general circulations. Izvestiya Atmos Ocean Phys. https://doi.org/10.1134/S000143381004002X

von Storch H, Zwiers FW (1984) Statistical analysis in climate research. https://doi.org/10.1017/cbo9780511612336

Watanabe S, Hajima T et al (2011) Miroc-esm 2010: model description and basic results of CMIP5-20C3M experiments. Geosci Model Dev. https://doi.org/10.5194/gmd-4-845-2011

Watanabe M, Suzuki T et al (2010) Improved climate simulation by miroc5: mean states, variability, and climate sensitivity. J Clim. https://doi.org/10.1175/2010JCLI3679.1

Watanabe M, Kamae Y, Shiogama H, DeAngelis AM, Suzuki K (2018) Low clouds link equilibrium climate sensitivity to hydrological sensitivity. Nat Clim Change. https://doi.org/10.1038/s41558-018-0272-0

Williamson MS, Thackeray CW, Cox PM, Hall A, Huntingford C, Nijsse FJ (2021) Emergent constraints on climate sensitivities. Rev Mod Phys. https://doi.org/10.1103/RevModPhys.93.025004

Wu T, Song L, Wea L (2014) An overview of bcc climate system model development and application for climate change studies. J Meteorol Res. https://doi.org/10.1007/s13351-014-3041-7

Wu T, Yu R, Lu Y (2021) BCC-CSM2-HR: a high-resolution version of the Beijing climate center climate system model. Geosci Model Dev 14(5):2977–3006. https://gmd.copernicus.org/articles/14/2977/2021/

Yukimoto S, Adachi Y et al (2012) A new global climate model of the meteorological research institute: MRI-CGCM3: model description and basic performance-. J Meteorol Soc Jpn. https://doi.org/10.2151/jmsj.2012-A02

Yukimoto S, Kawai H, Koshiro T (2019) The meteorological research institute earth system model version 2.0, MRI-ESM2.0: description and basic evaluation of the physical component. J Meteorol Soc Jpn. https://doi.org/10.2151/jmsj.2019-051

Zelinka MD, Myers TA, McCoy DT (2020) Causes of higher climate sensitivity in cmip6 models. Geophys Res Lett. https://doi.org/10.1029/2019GL085782

Ziehn T, Chamberlain MA, Law RM et al (2020) The Australian earth system model: access-ESM1.5. J Southern Hemisphere Earth Syst Sci. https://doi.org/10.1071/ES19035